Intermittency in ageing

2003 J. Phys.: Condens. Matter 15 S1163

(http://iopscience.iop.org/0953-8984/15/11/336)

INSTITUTE OF PHYSICS PUBLISHING JOURNAL OF PHYSICS: CONDENSED MATTER

J. Phys.: Condens. Matter **15** (2003) S1163–S1179 PII: S0953-8984(03)58212-1

Intermittency in ageing

L Buisson, L Bellon and S Ciliberto

Ecole Normale Supérieure de Lyon, Laboratoire de Physique, CNRS UMR5672,
46 Allée d'Italie, 69364 Lyon Cedex 07, France

Received 27 September 2002
Published 10 March 2003
Online at stacks.iop.org/JPhysCM/15/S1163

Abstract

The fluctuation–dissipation relation is measured on the dielectric properties of a gel (Laponite) and of a polymer glass (polycarbonate). For the gel it is found that during the transition from a fluid-like to a solid-like state the fluctuation–dissipation theorem is strongly violated. The amplitude and the persistence time of this violation are decreasing functions of frequency. Around 1 Hz it may persist for several hours. A very similar behaviour is observed in polycarbonate after a quench below the glass transition temperature. In both cases the origin of this violation is a highly intermittent dynamics characterized by large fluctuations. The relevance of these results for recent models of ageing is discussed.

(Some figures in this article are in colour only in the electronic version)

1. Introduction

Many systems in nature, such as glasses, spin-glasses, colloids and granular materials, present an extremely slow relaxation towards equilibrium and, when external conditions are modified, the physical properties of these materials evolve as a function of time: they are ageing. For example, when a glassy material is quenched from above its glass transition temperature T_g to a temperature lower than T_g, any response function of the material depends on the time t_w elapsed from the quench [1]. Another example of ageing is given by colloidal glasses, whose properties evolve during the sol–gel transition, which may last several days [2]. An important feature of ageing materials is the dependence of their physical properties on the thermal history of the sample. Indeed experimental procedures, based on multiple cycles of cooling, heating and waiting times, have shown the existence of two spectacular effects: memory and rejuvenation. Specifically, ageing materials perfectly recall their thermal history (*memory effect*). At the same time the low temperature state of these materials is independent of the complete cooling history (*rejuvenation*) and when the temperature is lowered the ageing may start again (see for example [3, 4] and references therein). Several models have been proposed to explain such a behaviour but from an experimental point of view it is not easy to distinguish between them. The above mentioned experimental procedures have, indeed,

been extremely useful to fix several constraints for the phenomenological models [5, 6], but these procedures are mainly based on the study of the response of the system to an external perturbation. Therefore they are unable to give new insight on the system dynamics. Let us consider for example the trap model [5] which is based on a phase space description. Its basic ingredient is an activation process and ageing is associated with the fact that deeper and deeper valleys are reached as the system evolves [7, 8]. The dynamics in this model has to be intermittent because either nothing moves or there is a jump between two traps [8]. This contrasts, for example, with mean field dynamics which is continuous in time [9]. Therefore, from an experimental point of view, it is extremely important to study not only the response of the system but also its thermal fluctuations. This analysis is also related to another important aspect of ageing dynamics, that is the definition of the temperature. Indeed recent theories [9] based on the description of spin glasses by a mean field approach proposed to extend the concept of temperature using a fluctuation–dissipation relation (FDR) which generalizes the fluctuation–dissipation theorem (FDT) for a weakly out of equilibrium system (for a review see [10–12]). In order to understand this generalization, we recall the main consequences of FDT in a system which is in thermodynamic equilibrium. We consider an observable V of such a system and its conjugate variable q. The response function $\chi_{Vq}(\omega)$, at frequency $f = \omega/2\pi$, describes the variation $\delta V(\omega)$ of V induced by a perturbation $\delta q(\omega)$ of q, that is $\chi_{Vq}(\omega) = \delta V(\omega)/\delta q(\omega)$. FDT relates the fluctuation spectral density of V to the response function χ_{Vq} and the temperature T of the system:

$$S(\omega) = \frac{2k_B T}{\pi\omega} \operatorname{Im}[\chi_{Vq}(\omega)] \tag{1}$$

where $S(\omega) = \langle |V(\omega)|^2 \rangle$ is the fluctuation spectral density of V, k_B is the Boltzmann constant and $\operatorname{Im}[\chi_{Vq}(\omega)]$ is the imaginary part of $\chi_{Vq}(\omega)$. Textbook examples of FDT are Nyquist's formula relating the voltage noise to the electrical resistance and the Einstein relation for Brownian motion relating the particle diffusion coefficient to the fluid viscosity [13].

When the system is not in equilibrium, FDT, that is equation (1), may fail. Indeed theoretical works [9] predict a violation of equation (1) which has been observed [10] in many numerical simulations [12, 14–20] and in a few experiments [21–25].

Because of the slow dependence on t_w of the response functions, it has been proposed to use an FDR which generalizes equation (1) and which can be used to define an effective temperature $T_{eff}(\omega, t_w)$ of the system [12]:

$$T_{eff}(\omega, t_w) = \frac{S(\omega, t_w)\pi\omega}{\operatorname{Im}[\chi_{Vq}(\omega, t_w)]2k_B}. \tag{2}$$

It is clear that if equation (1) is satisfied $T_{eff} = T$, otherwise T_{eff} turns out to be a decreasing function of t_w and ω. The physical meaning of equation (2) is that there is a timescale (for example t_w) which allows us to separate the fast processes from the slow ones. In other words the low frequency modes, such that $\omega t_w < 1$, relax towards the equilibrium value much more slowly than the high frequency ones which rapidly relax to the temperature of the thermal bath. Therefore it is conceivable that the low frequency modes keep memory of higher temperatures for a long time and for this reason their temperature should be higher than that of the high frequency ones. This striking behaviour has been observed in several numerical models of ageing [12, 14–20]. Further analytical and numerical studies of simple models show that equation (2) is a good definition of temperature in the thermodynamic sense [11, 12]. In spite of the large number of theoretical studies there are only a few experiments where FDR is studied in ageing materials. The experimental analysis of the dependence of $T_{eff}(\omega, t_w)$ on ω and t_w is very useful to distinguish among different models of ageing because the FDT

violations are model dependent [12, 14–20]. Furthermore the direct analysis of the noise signal allows one to understand if the dynamics is either intermittent or continuous in time.

Recently, a few experiments have analysed this problem in real materials [21–25]. The violation of FDT measured in an experiment on a spin glass [24] seems to be in agreement with theoretical predictions, which were originally based on the mean field approach of spin glasses. In contrast, experiments done on dielectric measurements on glycerol [21], colloidal glasses [22, 23] and polymers [25] present only a qualitative agreement with theory.

The previous analysis of colloidal glasses [22, 23] and of polycarbonate [25] was mainly based on the study of the time evolution of the noise spectra which is surprisingly similar in these two very different materials. In both cases the effective temperature defined using equation (2) is huge and the persistent time of the violation is extremely long. We have therefore analysed directly the time evolution of the noise signal in both experiments and we find a strongly intermittent behaviour in both materials. In this paper we describe the results of this analysis and we also want to point out the common features observed in the slow relaxation dynamics of these two materials.

The paper is organized as follows. In sections 2 and 3 we recall the main results of the experiments on the colloidal glass (Laponite) and polycarbonate respectively. We also describe the analysis performed on the time evolution of the noise signal. In section 4 we compare the results of the two experiments and we discuss their relevance for recent ageing models. Conclusions are given at the end of the section.

2. Laponite electric properties

We have experimentally studied FDR in Laponite during the transition from a fluid-like solution to a solid-like colloidal glass. The main control parameter of this transition is the concentration of Laponite[1], which is a synthetic clay consisting of discoid charged particles. It disperses rapidly in water to give gels even for very low mass fraction. Physical properties of this preparation evolve for a long time, even after the sol–gel transition, and have shown many similarities with standard glass ageing [2, 26]. Recent experiments [26] have even proved that the structure function of Laponite at low concentration ($<3\%$ mass fraction) is close to that of a glass. For this reason we call our gel a colloidal glass.

2.1. The experimental apparatus

The Laponite (see footnote 1) solution is used as a conductive liquid between the two gold coated electrodes of a cell (see figure 1). It is prepared in a clean N_2 atmosphere to avoid CO_2 and O_2 contamination, which perturbs the electrical measurements. Laponite particles are dissolved at a concentration of 2.5% mass fraction in pure water under vigorous stirring for 300 s. To avoid the existence of any initial structure in the sol, we pass the solution through a 1 μm filter when filling our cell. This instant defines the origin of the ageing time t_w (the filling of the cell takes roughly 2 min, which can be considered the maximum inaccuracy of t_w). The sample is then sealed so that no pollution or evaporation of the solvent can occur. At this concentration, the light scattering experiments show that Laponite (see footnote 1) structure functions are still evolving 500 h after the preparation [2]. We only study the beginning of this glass formation process.

The two electrodes of the cell are connected to our measurement system, where we alternately record the cell electrical impedance $Z(t_w, \omega)$ and the voltage noise density $S_Z(t_w, \omega)$

[1] Laponite RD is a registered trademark of Laporte Absorbents, PO Box 2, Cheshire, UK.

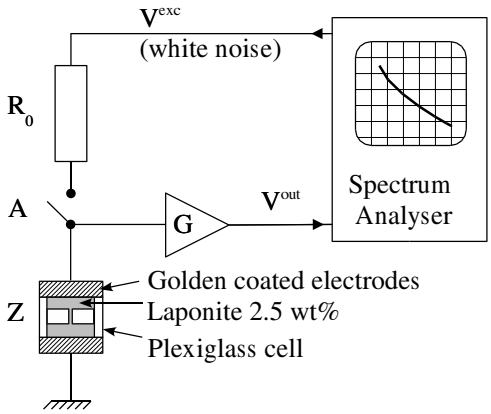

Figure 1. Laponite experimental set-up: the impedance under test Z is a cell filled with a 2.5 wt% Laponite sol. The cell is divided into two parts by a central wall. A rigid tube embedded in this wall connects two large reservoirs where the fluid is in contact with the electrodes which have an area of 25 cm^2 and are gold coated to avoid oxidation. The main contribution to the electrical resistance of the cell is given by the Laponite sol contained in the tube connecting the two reservoirs. One of the two electrodes is grounded whereas the other is connected to the input of a low noise voltage amplifier characterized by a voltage amplification G. With a spectrum analyser, we alternately record the frequency response $\mathrm{FR}(\omega) = \langle V^{out}/V^{exc}\rangle$ (switch A closed) and the spectrum $S(\omega) = \langle |V^{out}|^2\rangle$ (switch A opened). The input voltage V^{exc} is a white noise excitation, thus from $\mathrm{FR}(\omega)$ we derive the impedance $Z(\omega)$ as a function of ω, that is $Z(\omega) = R_0/(G/\mathrm{FR}(\omega) - 1)$; whereas from $S(\omega)$, we can estimate the voltage noise of Z, specifically $S_Z(\omega) = [S(\omega) - S_a(\omega)]/G^2$ where $S_a(\omega)$ is the noise spectral density of the amplifier.

(see figure 1). Taking into account that in this configuration $\mathrm{Im}[\chi_{Vq}(t_w, \omega)] = \omega\,\mathrm{Re}[Z(t_w, \omega)]$, one obtains from equation (2) that the effective temperature of the Laponite solution as a function of the ageing time and frequency is

$$T_{eff}(t_w, \omega) = \pi S_Z(t_w, \omega)/2k_B\,\mathrm{Re}[Z(t_w, \omega)] \tag{3}$$

which is an extension of the Nyquist formula.

The electrical impedance of the sample is the sum of two effects: the bulk is purely conductive, the ions of the solution follow the forcing field, whereas the interfaces between the solution and the electrodes give mainly a capacitive effect due to the presence of the Debye layer [27]. This behaviour has been validated using a four-electrode potentiostatic technique [28] to make sure that the capacitive effect is only due to the surface. In order to test only bulk properties, the geometry of the cell is tuned to push the surface contribution to low frequencies. As shown in the schematic diagram of figure 1, the cell is divided into two parts by a central wall. A rigid tube embedded in this wall connects two large reservoirs where the fluid is in contact with the electrodes which have an area of 25 cm^2. The main contribution to the electrical resistance of the cell is given by the Laponite sol contained in the tube connecting the two reservoirs. Thus by changing the length and the section of this tube the total bulk resistance of the sample can be changed from 300 Ω to 100 kΩ. We checked that the dynamics of the system does not depend on the value of the bulk resistance. For a bulk resistance of about 10^5 Ω the cut-off frequency of the equivalent *R–C* circuit (composed by the series of the Debye layers plus the bulk resistance) is about 0.02 Hz. In other words, above this frequency the imaginary part of the cell impedance is about zero.

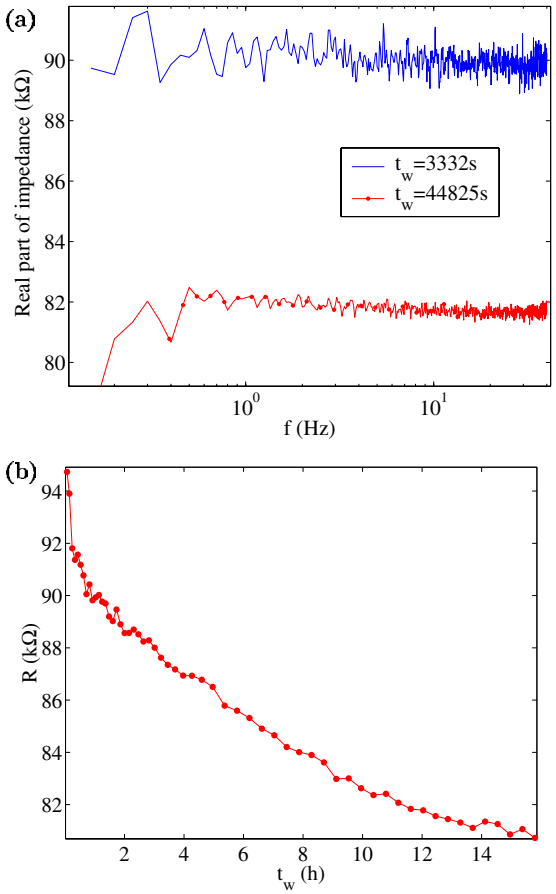

Figure 2. Laponite response function. (a) Frequency dependence of a sample impedance for two different ageing times: continuous curve $t_w = 3332$ s; ● $t_w = 44825$ s. (b) Time evolution of the resistance. This long time evolution is the signature of the ageing of the sol. In spite of the decreasing mobility of Laponite particles in solution during the gelation, the electrical conductivity increases.

2.2. FDR measurements in laponite

In figure 2(a), we plot the real part of the impedance as a function of the frequency f, for a typical experiment and two different times. The time evolution of the resistance of one of our samples is plotted in figure 2(b): it is still decaying in a non-trivial way after 24 h, showing that the sample has not reached any equilibrium yet. This ageing is consistent with that observed in light scattering experiments [2]. As the dissipative part of the impedance $\mathrm{Re}(Z)$ is weakly time and frequency dependent, one would expect from the Nyquist formula that so would be the voltage noise density S_Z. But, as shown in figure 3, FDR must be strongly violated for the lowest frequencies and earliest times of our experiment: S_Z changes by several orders of magnitude between the highest values and the high frequency tail[2]. This violation is clearly

[2] This low frequency noise cannot be confused with the standard $1/f$ noise observed in many electronic devices. We recall that the $1/f$ appears only when an external current produced by an external potential goes through the device. In our cell no external potential is applied.

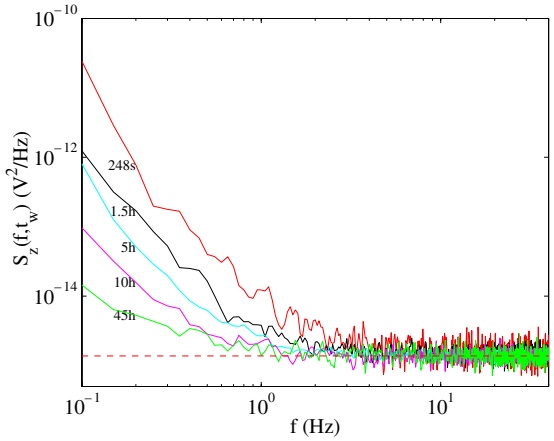

Figure 3. Voltage fluctuations for laponite: voltage noise density of one sample for different ageing times. The horizontal dashed line is the FDT prediction.

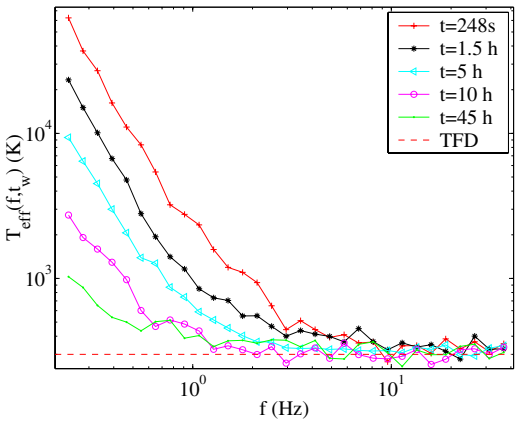

Figure 4. Effective temperature of laponite: effective temperature as a function of frequency for different ageing times. As for S_Z in figure 3, T_{eff} strongly increases and reaches huge values for low frequencies and short ageing times.

illustrated by the behaviour of the effective temperature in figure 4[3]. For long times and high frequencies, the FDR holds and the measured temperature is the room one (300 K), whereas for early times T_{eff} climbs up to 3×10^3 K at 1 Hz. Moreover, T_{eff} could be even larger for lower frequencies and lower ageing times: indeed, we did not find in any of the tested samples any evidence of a saturation of this effective temperature in our measurement range. In order to be sure that the observed violation is not due to an artifact of the experimental procedure, we filled the cell with an electrolyte solution with pH close to that of the Laponite sol such that the electrical impedance of the cell was the same. Specifically we filled the cell with NaOH solution in water at a concentration of 10^{-3} mol l^{-1}. The results of the measurements of T_{eff} are shown in figure 5 at two different times after the sample preparation. In this case we did not observe any violation of FDR at any time.

[3] The usual representation of the effective temperature in simulations is the slope of the response versus correlation plot, but it is not suited for our experimental data: the system being almost only dissipative, the response function is close to a delta distribution, thus FDR is only one point in this representation.

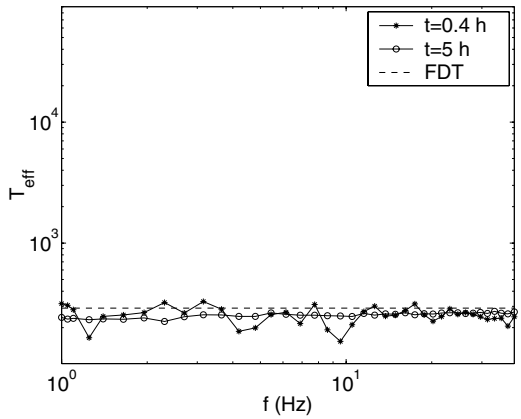

Figure 5. Effective temperature of an NaOH solution in water. The effective temperature is plotted as a function of frequency for two different times after the preparation. This solution has a pH close to that of the laponite, and no violation is observed in this case for any ageing time.

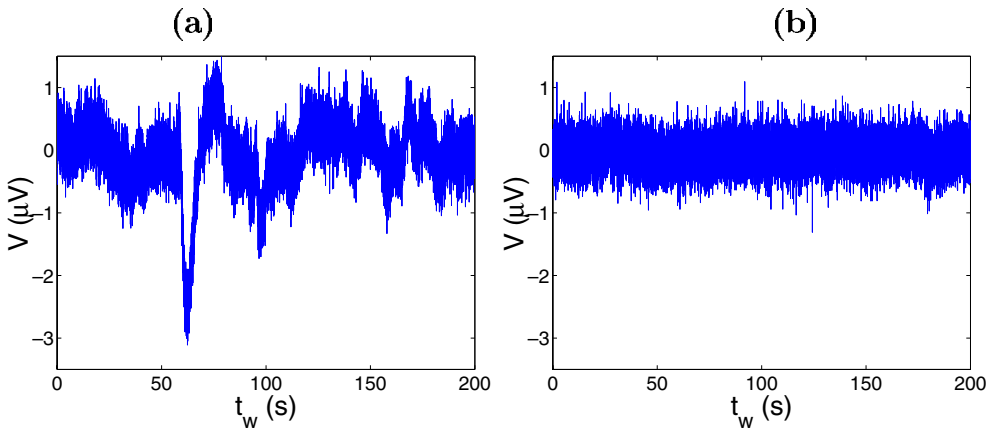

Figure 6. Voltage noise signal in laponite: (a) noise signal, 2 h after the Laponite preparation, when FDT is violated; (b) typical noise signal when FDT is not violated.

2.3. Statistical analysis of the noise

In order to understand such a behaviour we have directly analysed the noise voltage across the Laponite cell. This test can be safely done in our experimental apparatus because the amplifier noise is negligible with respect to the thermal noise of the Laponite cell even when FDT is satisfied. In figure 6(a) we plot a typical signal measured 2 h after the gel preparation when the FDT is strongly violated. The signal plotted in figure 6(b) has been measured when the system is relaxed and FDT is satisfied in the whole frequency range. By comparing the two signals we immediately realize that there are very important differences. The signal in figure 6(a) is interrupted by bursts of very large amplitude which are responsible for the increase of the noise in the low frequency spectra (see figure 3). The relaxation time of the bursts has no particular meaning, because it just corresponds to the characteristic time of the filter used to eliminate the very low frequency trends. As time goes on, the amplitude of the bursts reduces and the time between two consecutive bursts becomes longer and longer. Finally they disappear as

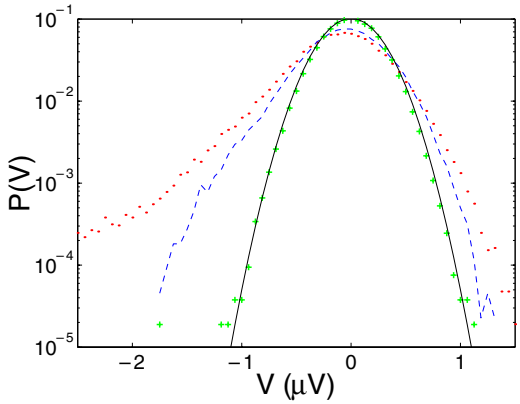

Figure 7. PDF of the voltage noise in laponite: typical PDF of the noise signal at different times after preparation, with, from top to bottom, $\cdots\cdots$ $t_w = 1$ h, - - - - $t_w = 2$ h and + $t_w = 50$ h. The continuous line is obtained from the FDT prediction.

can be seen in the signal of figure 6(b) recorded after 50 h when the system satisfies FDT. The evolution of the intermittent properties of the noise can be characterized by studying the probability density function (PDF) of the signal as a function of time. To compute the PDF, the time series are divided into several time windows and the PDF is computed in each of these windows. Afterwards, the result of several experiments are averaged. The PDF computed at different times is plotted in figure 7. We see that at short t_w the PDF presents very high tails which slowly disappear at longer t_w. Finally a Gaussian shape is recovered at $t_w = 16$ h. This kind of evolution of the PDF clearly indicates that the signal is very intermittent at the beginning and it relaxes to Gaussian noise at very long times.

The comparison of these results with ageing models will be presented in the conclusions. We prefer to describe now another experiment in a completely different material.

3. Polycarbonate dielectric properties

In order to give more insight into the problem of the violation of FDT and of the intermittent behaviour discussed in the previous section we have carried out wide band (20 mHz–100 Hz) measurements of the dielectric susceptibility and of the polarization noise in a polymer glass: polycarbonate. We present in this paper several results which show a strong violation of the FDT when this material is quenched from the molten state to below its glass-transition temperature. The effective temperature defined by equation (2) slowly relaxes towards the bath temperature. The violation is observed even at $\omega t_w \gg 1$ and it may last for more than 3 h for $f > 1$ Hz.

3.1. The experimental apparatus

The polymer used in this investigation is Makrofol DE 1-1 C, a bisphenol A polycarbonate, with $T_g \simeq 419$ K, produced by Bayer in the form of foils. We have chosen this material because it has a wide temperature range of strong ageing [1]. This polymer is totally amorphous: there is no evidence of crystallinity [29]. Nevertheless, the internal structure of polycarbonate changes and relaxes as a result of a change in the chain conformation by molecular motions [1, 30, 31]. Many studies of the dielectric susceptibility of this material exist, but none had an interest in the problem of noise measurements.

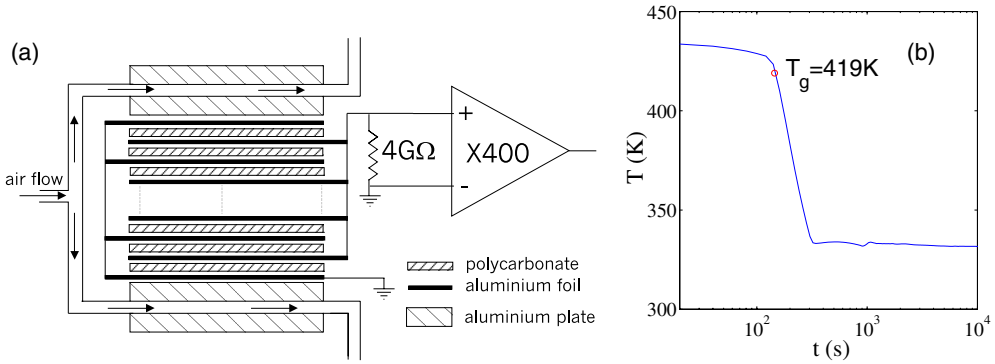

Figure 8. (a) Polycarbonate experimental set-up; (b) typical temperature quench: from $T_i = 433$ K to $T_f = 333$ K, the origin of t_w is at $T = T_g$.

In our experiment polycarbonate is used as the dielectric of a capacitor. The capacitor is composed by 14 cylindrical capacitors in parallel in order to reduce the resistance of the sample and to increase its capacity. Each capacitor is made of two aluminium electrodes, 12 μm thick, and by a disk of polycarbonate of diameter 12 cm and thickness 125 μm. The experimental set-up is shown in figure 8(a). The 14 capacitors are sandwiched together and put between two thick aluminium plates which contain an air circulation used to regulate the sample temperature. This mechanical design of the capacitor is very stable and gives very reproducible results even after many temperature quenches. The capacitor is inside two Faraday screens to insulate it from external noise. The temperature of the sample is controlled within a few per cent. Fast quench of about 50 K min^{-1} is obtained by injecting nitrogen vapour in the air circulation of the aluminium plates. The electrical impedance of the capacitor is $Z(\omega, t_w) = R/(1+\mathrm{i}\omega RC)$, where C is the capacitance and R is a parallel resistance which accounts for the complex dielectric susceptibility. It is measured using a Novocontrol dielectric analyser. The noise spectrum of this impedance $S_Z(\omega, t_w)$ is

$$S_Z(f, t_w) = 4k_B T_{eff}(f, t_w)\,\mathrm{Re}[Z(\omega, t_w)] = \frac{4k_B T_{eff}(f, t_w)R}{1 + (\omega RC)^2} \tag{4}$$

where T_{eff} is the effective temperature of the sample. In order to measure $S_Z(f, t_w)$, we have made a differential amplifier based on selected low noise JFET (2N6453 InterFET corporation), whose input has been polarized by a resistance $R_i = 4$ GΩ. Above 2 Hz, the input voltage noise of this amplifier is 5 nV(Hz)$^{-1/2}$ and the input current noise is about 1 fA(Hz)$^{-1/2}$. The output signal of the amplifier is analysed either by an HP3562A dynamic signal analyser or directly acquired by a NI4462 card. It is easy to show that the measured spectrum at the amplifier input is

$$S_V(f, t_w) = \frac{4k_B RR_i(T_{eff}(f, t_w)R_i + T_R R + S_\xi(f)RR_i)}{(R + R_i)^2 + (\omega RR_i C)^2} + S_\eta(f) \tag{5}$$

where T_R is the temperature of R_i and S_η and S_ξ are respectively the voltage and the current noise spectrum of the amplifier. In order to reach the desired statistical accuracy of $S_V(f, t_w)$, we averaged the results of many experiments. In each of these experiments the sample is first heated to $T_i = 433$ K. It is maintained at this temperature for 4 h in order to reinitialize its thermal history. Then it is quenched from T_i to $T_f = 333$ K in about 2 min. A typical thermal history of the quench is shown in figure 8(b). The reproducibility of the capacitor impedance during this thermal cycle is always better than 1%. The origin of ageing time t_w is the instant

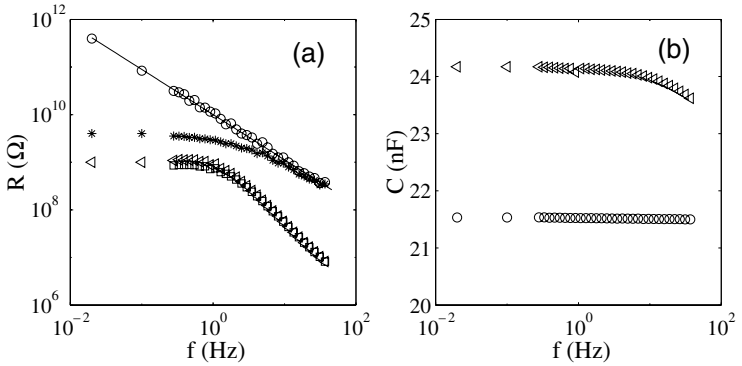

Figure 9. Polycarbonate response function. (a) Polycarbonate resistance R as a function of frequency measured at $T_i = 433$ K (◁) and at $T_f = 333$ K (○). The effect of the 4 GΩ input resistance is also shown at $T = 433$ K (□) and at $T = 333$ K (∗). (b) Polycarbonate capacitance versus frequency measured at $T_i = 433$ K (◁) and at $T_f = 333$ K (○).

when the capacitor temperature is at $T_g \simeq 419$ K, which of course may depend on the cooling rate. However, adjustment of T_g by a few degrees will shift the time axis by at most 30 s, without affecting our results.

3.2. FDR measurements

In figures 9(a) and (b), we plot the measured values of R and C as a function of f at T_i and at T_f for $t_w \geqslant 200$ s. We see that on lowering temperature R increases and C decreases. At T_f ageing is small and extremely slow. Thus for $t_w > 200$ s the impedance can be considered constant without affecting our results. From the data plotted in figures 9(a) and (b) one finds that $R = 10^{10}(1 \pm 0.05) f^{-1.05\pm0.01}$ Ω and $C = (21.5 \pm 0.05)$ nF. In figure 9(a) we also plot the total resistance at the amplifier input which is the parallel of the capacitor impedance with R_i. We see that at T_f the input impedance of the amplifier is negligible for $f > 10$ Hz, whereas it has to be taken into account at lower frequencies.

Figure 10(a) represents the evolution of $S_V(f, t_w)$ after a quench. Each spectrum is obtained as an average in a time window starting at t_w. The time window increases with t_w so to reduce error for large t_w. Then the results of seven quenches have been averaged. For the longest time ($t_w = 1$ day) the equilibrium FDT prediction (continuous line) is quite well satisfied. We clearly see that FDT is strongly violated for all frequencies at short times. Then high frequencies relax on the FDT, but there is a persistence of the violation for lower frequencies. The amount of the violation can be estimated by the best fit of $T_{eff}(f, t_w)$ in equation (5) where all other parameters are known. We started at very large t_w when the system is relaxed and $T_{eff} = T$ for all frequencies. Inserting the values in equation (5) and using the S_V measured at $t_w = 1$ day we find $T_{eff} \simeq 333$ K, within error bars for all frequencies (see figure 10(b)). At short t_w, data show that $T_{eff}(f, t_w) \simeq T_f$ for f larger than a cut-off frequency $f_o(t_w)$ which is a function of t_w. In contrast, for $f < f_o(t_w)$ we find that T_{eff} is $T_{eff}(f, t_w) \propto f^{-A(t_w)}$, with $A(t_w) \simeq 1$. This frequency dependence of $T_{eff}(f, t_w)$ is quite well approximated by

$$T_{eff}(f, t_w) = T_f \left[1 + \left(\frac{f}{f_o(t_w)} \right)^{-A(t_w)} \right] \tag{6}$$

where $A(t_w)$ and $f_o(t_w)$ are the fitting parameters. We find that $1 < A(t_w) < 1.2$ for the whole data set. Furthermore, for $t_w \geqslant 250$, it is enough to keep $A(t_w) = 1.2$ to fit the data within

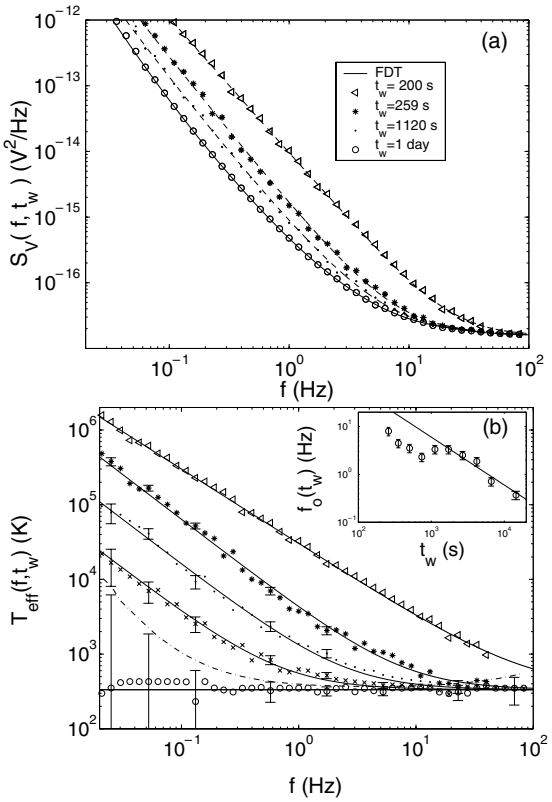

Figure 10. Voltage noise and effective temperature in polycarbonate. (a) Noise power spectral density $S_V(f, t_w)$ measured at $T_f = 333$ K and different t_w. The spectra are the averages over seven quenches. The continuous curve is the FDT prediction. Dashed curves are the fits obtained using equations (5) and (6) (see the text for details). (b) Effective temperature versus frequency at $T_f = 333$ K for different ageing times: $\lhd\, t_w = 200$ s, $*\, t_w = 260$ s, $\bullet\ t_w = 2580$ s, $\times\ t_w = 6542$ s and $\mathrm{O}\ t_w = 1$ day. The continuous curves are the fits obtained using equation (6). The horizontal straight line is the FDT prediction. The dot–dashed curve corresponds to the limit where the FDT violation can be detected. In the inset the frequency $f_o(t_w)$, defined in equation (6), is plotted as a function of t_w. The continuous line is not a fit, but it corresponds to $f_o(t_w) \propto 1/t_w$.

error bars. For $t_w < 250$ s we fixed $A(t_w) = 1$. Thus, the only free parameter in equation (6) is $f_o(t_w)$. The continuous curves in figure 10 (a) are the best fits of S_V found by inserting equation (6) in (5).

In figure 10(b) we plot the estimated $T_{eff}(f, t_w)$ as a function of frequency at different t_w. We see that just after the quench $T_{eff}(f, t_w)$ is much larger than T_f in the whole frequency interval. High frequencies rapidly decay towards the FDT prediction whereas at the smallest frequencies $T_{eff} \simeq 10^5$ K. Moreover we notice that low frequencies decay more slowly than high frequencies and that the evolution of $T_{eff}(f, t_w)$ towards the equilibrium value is very slow. From the data of figure 10(b) and equation (6), it is easy to see that $T_{eff}(f, t_w)$ can be superposed onto a master curve by plotting it as a function of $f/f_o(t_w)$. The function $f_o(t_w)$ is a decreasing function of t_w, but the dependence is not a simple one, as can be seen in the inset of figure 10(b). The continuous straight line is not fitted; it represents $f_o(t_w) \propto 1/t_w$ which seems a reasonable approximation for these data. For $t_w > 10^4$ s we find $f_o < 1$ Hz. Thus we cannot follow the evolution of T_{eff} any longer because the contribution of the experimental

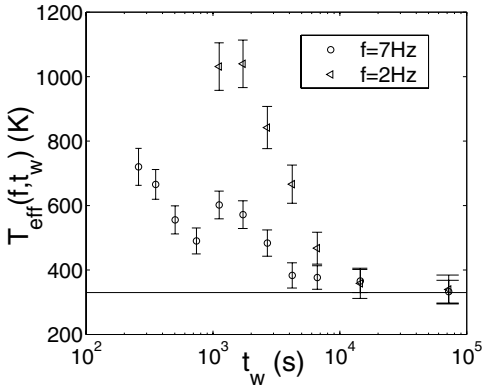

Figure 11. Violation of FDT in polycarbonate: effective temperature at 7 Hz (○) and 2 Hz (◁) measured as a function of t_w at $T_f = 333$ K.

noise on S_V is too big, as shown in figure 10(b) by the increasing of the error bars for $t_w = 1$ day and $f < 0.1$ Hz.

Before discussing these experimental results we want to compare them to the single-frequency experiment performed on glycerol [21]. In this experiment, T_{eff} has been measured only at 7 Hz. Thus, we studied how $T_{eff}(7\text{ Hz}, t_w)$ depends on t_w at 7 Hz in our experiment. The time evolution of $T_{eff}(7\text{ Hz}, t_w)$ is plotted as a function of t_w in figure 11. The time evolution of $T_{eff}(2\text{ Hz}, t_w)$ is also plotted just to show the large temperature difference between the two frequencies. Let us consider the evolution at 7 Hz only. As in the experiment of [21], we confirm the fact that the violation is observed even if $\omega t_w \gg 1$, which is in contrast with theoretical predictions. The biggest violation is for short times after the quench where the effective temperature is surprisingly huge: around 800 K at 7 Hz and $t_w = 300$ s. In the experiment on glycerol the first data reported are for $t_w > 1000$ s. Thus if we consider only data at $t_w > 1000$ s in figure 11 we see that our results are close to those of [21]. Indeed at $t_w = 1000$ s we find in our experiment $(T_{eff} - T_f)/(T_g - T_f) \simeq 2.4$, the glycerol data give $(T_{eff} - T_f)/(T_g - T_f) \simeq 1$. Thus the relative violations of FDT at 7 Hz are very close in glycerol and polycarbonate. However it would be interesting to check whether at shorter times and at lower frequencies large T_{eff} could be observed in glycerol too.

In order to compare with theoretical predictions [9, 12] and a recent spin glass experiment [24] we may plot the integrated response $R(t, t_w)$ as a function of the correlation $C(t, t_w)$. The latter is obtained by inserting the measured $T_{eff}(f, t_w)$ in equation (4) and by Fourier transforming this equation. $R(t, t_w)$ can be computed by Fourier transforming $Real[Z(\omega, t_w)]$. FDR now takes the form [12]

$$-C(t, t_w) + C(t_w, t_w) = k_B T_{eff}(t, t_w) R(t, t_w). \tag{7}$$

In figure 12(a), we see that for $t_w > 300$ s the shape of the decay of $C(t_w, t)$ remains essentially the same. Indeed data for different t_w can be scaled onto a single master curve by plotting $C(t_w, t)$ as a function $(t - t_w)/t_o(t_w)$, where $t_o(t_w)$ is an increasing function of t_w plotted in the inset of figure 12. For $t_w > 200$ s, $t_o(t_w)$ is very close to $1/f_o(t_w)$, where $f_o(t_w)$ is the T_{eff} cut-off frequency obtained from equation (6). The self-similarity of correlation functions, found on our dielectric data, is a characteristic of the universal picture of ageing [10, 12, 15, 16, 32], which has also been observed in a spin-glass experiment [24] and in the structure function of the dynamic light scattering of colloidal gels [33]. Thus our results confirm that this picture of ageing also applies to the polymer

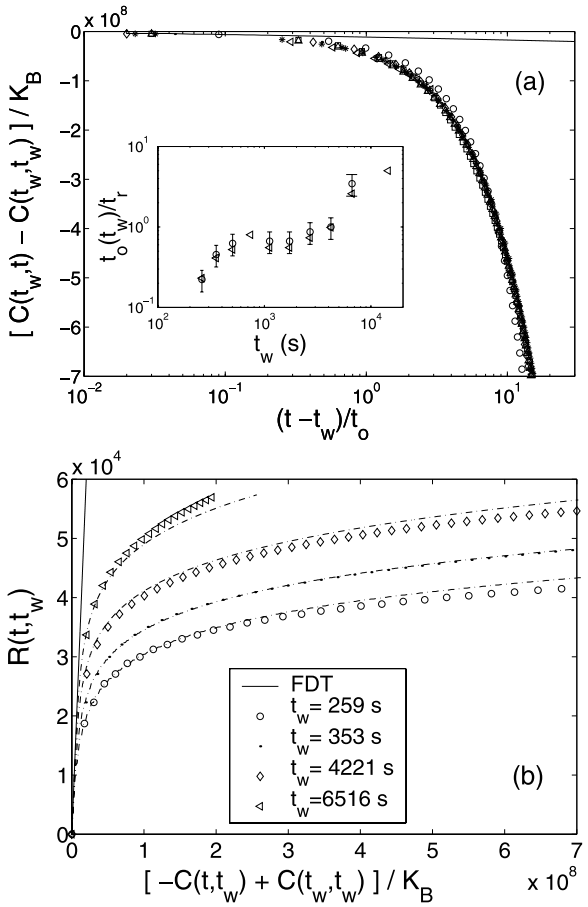

Figure 12. (a) The correlation function $C(t, t_w) - C(t_w, t_w)$ is plotted as a function of time for several t_w, specifically ○ $tw = 259$ s, ● $t_w = 353$ s, ◇ $t_w = 4221$ s and ◁ $t_w = 6516$ s. The continuous curve is the FDT prediction. The correlation functions have been superposed by scaling $t - t_w$ by a characteristic time $t_o(t_w)$ which is an increasing function of t_w. In the inset $t_o(t_w)/t_r$ (○) is plotted as a function of t_w, with $t_r = t_o$ (4220 s). The values of $f_o(4220s)/f_o(t_w)$ (◁) are also plotted. The characteristic frequency estimated from the spectra (equation (6)) is equal, within error bars, to the inverse of characteristic time obtained from the superposition of the correlation function. (b) Plot of the integrated response $R(t, t_w)$ as a function of $-C(t, t_w) + C(t_w, t_w)$ at different t_w. Symbols correspond to the data: ○ $tw = 259$ s, ● $t_w = 353$ s, ◇ $t_w = 4221$ s and ◁ $t_w = 6516$ s. The dashed curves are obtained from the best fits (see the text for details). The continuous curve is the FDT prediction.

dielectric measurements. To further investigate this ageing, we plot, in figure 12(b), $R(t, t_w)$ as a function $(-C(t, t_w) + C(t_w, t_w))/k_B$ at different t_w. The slope of this graph gives $1/T_{eff}$. The symbols correspond to the data whereas the dashed curves are obtained by inserting the best fit of T_{eff} into equations (6) and (4). We clearly see that data at small $C(t, t_w)$ asymptotically converge to a horizontal straight line, which means that the system has an infinite temperature. At short time, large $C(t, t_w)$, the FDT prediction is recovered (continuous straight line of slope $1/T_f$). This result is quite different to what has been observed in recent experiments on spin glasses where $T_{eff} \simeq 5T_g$ has been measured [24]. In contrast infinite T_{eff} has been observed during the sol–gel transition [22] and in numerical simulation of domain growth phenomena [17].

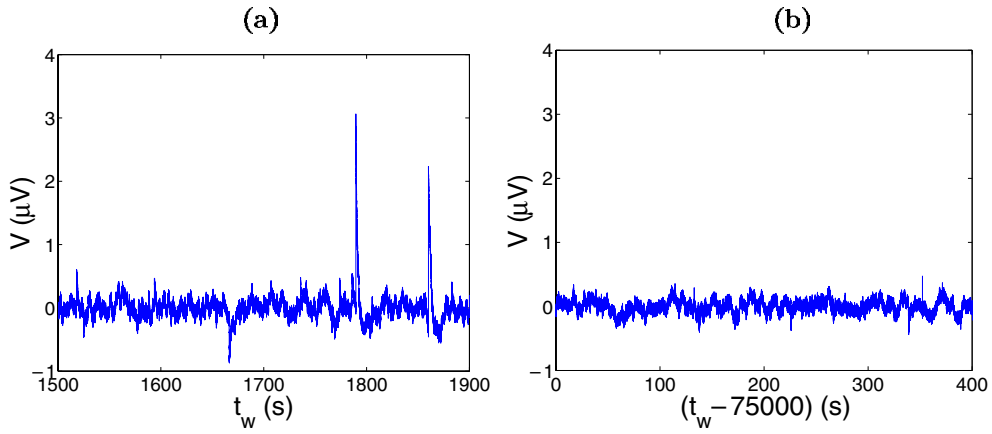

Figure 13. Voltage noise signal in polycarbonate: typical noise signal of polycarbonate measured at 1500 s $< t_w <$ 1900 s (a) and $t_w >$ 75 000 s (b).

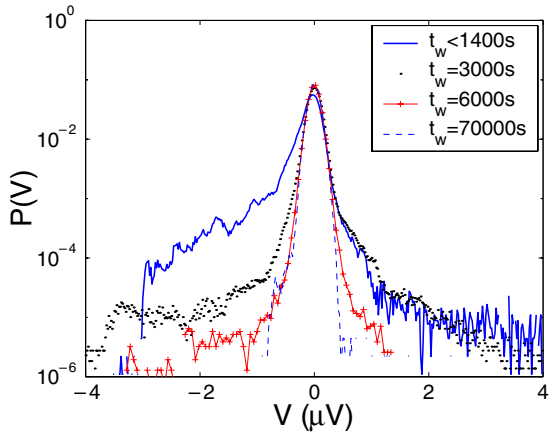

Figure 14. PDF of voltage noise in polycarbonate: typical PDF of the noise signal of polycarbonate measured at various t_w.

3.3. Statistical analysis of the noise

In order to understand the origin of such large deviations in our experiment we have analysed the noise signal. We find that the signal is characterized by large intermittent events which produce low frequency spectra proportional to $f^{-\alpha}$ with $\alpha \simeq 2$. Two typical signals recorded at 1500 s $< t_w <$ 1900 s and $t_w >$ 75 000 s are plotted in figure 13. We clearly see that in the signal recorded at 1500 s $< t_w <$ 1900 s there are very large bursts which are at the origin of the frequency spectra discussed in the previous section. In contrast in the signal (figure 13(b)), which was recorded at $t_w >$ 75 000 s when FDT is not violated, the bursts have totally disappeared.

As for Laponite we have studied the PDF of the signal as a function of t_w for polycarbonate. The results are shown in figure 14. We clearly see that the PDF, measured at small t_w, has very high tails which become smaller and smaller at large t_w. Finally the Gaussian profile is recovered after 24 h. This strongly intermittent dynamics is reminiscent of the intermittence observed in the local measurements of polymer dielectric properties [34] and in the slow relaxation dynamics of a colloidal gel [35].

4. Discussion and conclusions

Let us review the main results of the two experiments described in the previous sections. We have seen that dielectric measurements of Laponite, during the sol–gel transition, and of polycarbonate, after a temperature quench, show a strong violation of FDT. In agreement with theoretical prediction the amplitude and the persistence time of the FDT violation is a decreasing function of frequency and time. The effective temperature defined by equation (2) is huge at small f and t_w and slowly relaxes towards the bath temperature. In contrast to theoretical predictions the violation is observed even at $\omega t_w \gg 1$ and it may last for more than 3 h for $f > 1$ Hz. We have then investigated the behaviour of the noise signals and we have shown that the huge T_{eff} is produced by very large intermittent bursts which are at the origin of the low frequency power law decay of noise spectra. Furthermore we have also shown that for both materials the statistics of this event is strongly non-Gaussian when FDT is violated and slowly relaxes to a Gaussian one at very long t_w. Thus these two very different materials have a very similar relaxation dynamics, characterized by a strong intermittency. This strongly intermittent dynamics is reminiscent of the intermittence observed in the local measurements of polymer dielectric properties [34]. Furthermore recent measurements made, using time resolved correlation in diffusing wave spectroscopy, have shown a strong intermittency in the slow relaxation dynamics of a colloidal gel [35].

The first striking result which merits discussion is the huge T_{eff} measured in Laponite and polycarbonate. Such a large T_{eff} is not specific to our systems but has been observed in domain growth models [12, 17] and in models controlled by activation processes [8, 36]. The question is whether these models may have some connections with our observations. We have seen that in our experiments the high effective temperature is produced by a very intermittent dynamics. This kind of behaviour can, indeed, be interpreted on the basis of the trap model [5, 8], which predicts non-trivial violation of FDT associated with an intermittent dynamics. The system evolves in deeper and deeper valleys on the energy landscape. The dynamics is fundamentally intermittent because either nothing moves or there is a jump between two traps. In our case these jumps could explain the presence in the dielectric voltage noise of very large and rare peaks with a slow relaxation after the jump. Clear answers to this question can be given by a detailed study of the statistics of the time intervals between large peaks. This study is in progress.

This paper clearly shows the importance of associating thermal noise and response measurements. As we have already pointed out in the introduction the standard techniques, based on response measurements and on the application of thermal perturbations to the sample, are certainly important to fix several constraints for the phase space of the system. However, they do not give information on the dynamics of the sample, which can be obtained by the study of FDR.

Many questions remain open on the subject of FDR in out of equilibrium systems. One may wonder whether different couples of conjugated variables give the same T_{eff} as defined by equation (2). For example FDR measured on the rheological properties of Laponite shows no violation of FDT [23]. From a theoretical viewpoint it has been shown that T_{eff} may depend on the observable in models controlled by an activation process [8, 36] such as the trap model, where T_{eff} can be huge or even infinite for several observables and much smaller for others. This analogy on the observable dependence of T_{eff} reinforces the description in terms of trap model of the ageing dynamics of our Laponite samples. However the reason for the difference between electrical and mechanical measurements in our Laponite samples is unclear and much work is necessary to give more insight into these problems.

Acknowledgments

We acknowledge useful discussion with J Kurchan and J P Bouchaud, who is also thanked for useful comments on the manuscript. We thank P Metz and F Vittoz for technical support. This work has been partially supported by the Région Rhône-Alpes contract 'Programme thématique: Vieillissement des matériaux amorphes'.

References

[1] Struik L C 1978 *Physical Aging in Amorphous Polymers and Other Materials* (Amsterdam: Elsevier)
[2] Kroon M, Wegdam G H and Sprik R 1996 Dynamic light scattering studies on the sol–gel transition of a suspension of anisotropic colloidal particles *Phys. Rev.* E **54** 1
[3] Jonason K, Vincent E, Hammann J and Bouchaud J P 1998 Memory and chaos effects in spin glasses *Phys. Rev. Lett.* **81** 3243
[4] Bellon L, Ciliberto S and Laroche C 2002 Advanced memory effects in the aging of a polymer glass *Eur. Phys. J.* B **25** 223
[5] Bouchaud J P and Dean D S 1995 Aging on Parisi's tree *J. Physique* I **5** 265
[6] Fisher D S and Huse D A 1986 Ordered phase of short range Ising spin-glasses *Phys. Rev. Lett.* **56** 1601
Fisher D S and Huse D A 1988 Nonequilibrium dynamics in spin glasses *Phys. Rev.* B **38** 373
[7] Bertin E and Bouchaud J P 2002 Dynamical ultrametricity in the critical trap model *J. Phys. A: Math. Gen.* **35** 3039 (*Preprint* cond-mat/0112187)
[8] Fielding S and Sollich P 2002 Observable dependence of fluctuation dissipation relation and effective temperature *Phys. Rev. Lett.* **88** 50603-1
[9] Cugliandolo L and Kurchan J 1993 Analytical solution of the off equilibrium dynamics of a long range spin glass model *Phys. Rev. Lett.* **71** 173
[10] Bouchaud J P, Cugliandolo L F, Kurchan J and Mézard M 1998 Out of equilibrium dynamics in spin glasses and other glassy systems *Spin Glasses and Random Fields* ed A P Young (Singapore: World Scientific) (*Preprint* cond-mat/9702070)
[11] Cugliandolo L 1998 Effective temperatures out of equilibrium *Trends in Theoretical Physics* vol 2, ed H Falomir *et al Am. Inst. Phys. Conf. Proc. 1998 Buenos Aires Mtg* (*Preprint* cond-mat/9903250)
[12] Cugliandolo L, Kurchan J and Peliti L 1997 Energy flow, partial equilibration and effective temperatures in systems with slow dynamics *Phys. Rev.* E **55** 3898
[13] de Groot S R and Mazur P 1984 *Non Equilibrium Thermodynamics* (New York: Dover)
[14] Parisi G 1997 Off-equilibrium fluctuation–dissipation relation in fragile glasses *Phys. Rev. Lett.* **79** 3660
[15] Kob W and Barrat J L 1997 Aging effects in a Lennard-Jones glass *Phys. Rev. Lett.* **78** 4581
[16] Barrat J L and Kob W 1999 Fluctuation dissipation ratio in an aging Lennard-Jones *Europhys. Lett.* **46** 637
[17] Barrat A 1998 Monte-Carlo simulations of the violation of the fluctuation–dissipation theorem in domain growth processes *Phys. Rev.* E **57** 3629
[18] Sellitto M 1998 Fluctuation dissipation ratio in lattice-gas models with kinetic constraints *Eur. Phys. J.* B **4** 135
[19] Marinari E, Parisi G, Ricci-Tersenghi F and Ruiz-Lorenzo J J 1998 Violation of the fluctuation dissipation theorem in finite dimensional spin glasses *J. Phys. A: Math. Gen.* **31** 2611
[20] Berthier L, Barrat J L and Kurchan J 2000 Two-times scales, two temperature scenario for nonlinear rheology *Phys. Rev.* E **61** 5464
[21] Grigera T S and Israeloff N 1999 Observation of fluctuation–dissipation-theorem violations in a structural glass *Phys. Rev. Lett.* **83** 5038
[22] Bellon L, Ciliberto S and Laroche C 2001 Violation of fluctuation dissipation relation during the formation of a colloidal glass *Europhys. Lett.* **53** 511
[23] Bellon L and Ciliberto S 2002 Experimental study of fluctuation dissipation relation during the aging process *Physica* D **168** 325
[24] Herisson D and Ocio M 2002 Fluctuation–dissipation ratio of a spin glass in the aging regime *Phys. Rev. Lett.* **88** 257702 (*Preprint* cond-mat/0112378)
[25] Buisson L, Garcimartin A and Ciliberto S 2003 submitted
[26] Bonn D, Tanaka H, Wegdam G, Kellay H and Meunier J 1999 Aging of a colloidal 'Wigner' glass *Europhys. Lett.* **45** 52
Bonn D, Kellay H, Tanaka H, Wegdam G and Meunier J 1999 *Langmuir* **15** 7534
[27] Hunter R 1989 *The Foundation of Colloid Science* (Oxford: Clarendon Press)
[28] Koryta J, Dvorak L and Kavan L 1993 *Principles of Electrochemistry* 2nd edn (New York: Wiley)

[29] Robertson C G and Wilkes G L 2000 Long term volume relaxation of bisphenol A polycarbonate and atactic polystyrene *Macromolecules* **33** 3954
[30] Saviot L, Duval E, Jal J F and Dianoux A J 2000 Very fast relaxation in polycarbonate glass *Eur. Phys. J.* B **17** 661
[31] Quinson R 1998 Caractérisation et modlisation de la déformation non élastique des polyméres amorphes á l'état solide *PhD Thesis* INSA
[32] Berthier L and Bouchaud J P 2002 Geometrical aspects of aging and rejuvenation in the Ising spin glass: a numerical study *Phys. Rev.* B **66** 054404
(Berthier L and Bouchaud J P 2002 *Preprint* cond-mat/0202069v1)
[33] Cipelletti L, Manley S, Ball R C and Weitz D A 2000 Universal aging features in the restructuring of fractal colloidal gels *Phys. Rev. Lett.* **84** 2275
[34] Vidal Russel E and Israeloff N E 2000 Direct observation of molecular cooperativity near the glass transition *Nature* **408** 695
[35] Cipelletti L, Bissig H, Trappe V, Ballestat P and Mazoyer S 2003 *J. Phys.: Condens. Matter* **15** S257
[36] Perez-Madrid A, Reguera D and Rubi J M 2002 Origin of the violation of the fluctuation–dissipation theorem in systems with activated dynamics
(Perez-Madrid A, Reguera D and Rubi J M 2002 *Preprint* cond-mat/0210089)